Published in final edited form as:
J Cell Physiol. 2010 November ; 225(2): 390–393. doi:10.1002/jcp.22280.

Cancer Hallmarks in Induced Pluripotent Cells: New Insights

Sergey Malchenko[1], **Vasil Galat**[2], **Elisabeth A. Seftor**[1], **Elio F. Vanin**[1], **Fabricio F. Costa**[1], **Richard E.B. Seftor**[1], **Marcelo B. Soares**[2], and **Mary J.C. Hendrix**[1,*]

[1]Cancer Biology and Epigenomics, Children's Memorial Research Center, Northwestern University, Feinberg School of Medicine, Chicago, IL 60614, USA

[2]Developmental Biology, Children's Memorial Research Center, Northwestern University, Feinberg School of Medicine, Chicago, IL 60614, USA

Abstract

Studies are beginning to emerge that demonstrate intriguing differences between human induced pluripotent stem cells (hiPSCs) and human embryonic stem cells (hESCs). Here, we investigated the expression of key members of the Nodal embryonic signaling pathway, critical to the maintenance of pluripotency in hESCs. Western blot and Real-time RT-PCR analyses reveal slightly lower levels of Nodal (a TGF-β family member) and Cripto-1 (Nodal's co-receptor) and a dramatic decrease in Lefty (Nodal's inhibitor and TGF-β family member) in hiPSCs compared with hESCs. The noteworthy drop in hiPSC's Lefty expression correlated with an increase in the methylation of *Lefty B* CpG island. Based on these findings, we addressed a more fundamental question related to the consequences of epigenetically reprogramming hiPSCs, especially with respect to maintaining a stable ESC phenotype. A global comparative analysis of 365 microRNAs (miRs) in two hiPSC *vs*. four hESC lines ultimately identified 10 highly expressed miRs in hiPCSs with >10-fold difference, which have been shown to be cancer related. These data demonstrate cancer hallmarks expressed by hiPSCs, which will require further assessment for their impact on future therapies.

The technologies developed to produce induced human pluripotent stem cells (hiPSCs), derived by epigenetic reprogramming of human fibroblasts, have provided an exciting new platform for generating dedifferentiated somatic cells -- thought to be almost identical to human embryonic stem cells (hESCs) (Yu et al., 2007) and of great promise for patient-tailored regenerative medicine therapies. However, recent reports are beginning to highlight noteworthy differences in gene expression signatures (Chin et al., 2009) and differential DNA methylation patterns (Doi et al., 2009) between these two stem cell types that collectively prompt additional comparative analyses. Equally important is the challenge we face in the scientific community promoting the use of embryonic stem cells, for regenerative medicine therapies, fully recognizing their tumorigenic potential in immunocompromised mouse models and our lack of understanding how to regulate normal pluripotency and differentiation over tumorigenic potential (reviewed by Knoepfler, 2009). Therefore, the aim of our study was to initially assess the expression levels of three major components of the embryonic Nodal signaling pathway, which is of critical significance in stem cell pluripotency and differentiation (Schier, 2003). Nodal is a member of the TGF-β family and an important morphogen and regulator of cell fate in embryological systems and requires tight control of its biological function (Schier and Shen, 200). Extracellular Nodal inhibitors, such as Lefty A and Lefty B (divergent members of the TGF-β family), control Nodal signaling by binding directly to Nodal, or by binding to Cripto-1 (Nodal's co-receptor and a

*Correspondence to: Mary J.C. Hendrix, Children's Memorial Research Center, 2430 N. Halsted St., Chicago, Illinois 60614., m-hendrix@northwestern.edu.

member of the Epidermal Growth Factor-Cripto-1/FRL-1/Cryptic [EGF-CFC] family). Our results demonstrate lower levels of Nodal (a TGF-β family member) and Cripto-1 (Nodal's co- receptor) and a dramatic decrease in Lefty (Nodal's inhibitor and TGF-β family member) in hiPSCs compared with hESCs (with an accompanying increase in the methylation of *Lefty B* CpG island). Based on these findings, the second part of our study addressed the implications associated with the epigenetic reprogramming of hiPSCs, consisting of a global comparative analysis of 365 microRNAs (miRs) in hiPSC *vs*. hESC lines. The data reveal 10 highly expressed miRs in hiPSCs with >10-fold difference, which have been shown to be cancer related, thus serving as a catalyst for further assessment with respect to their clinical use in regenerative medicine.

MATERIALS AND METHODS

Cells and culture

Two hiPSC cultures IMR90-1, Foreskin -1 (WiCell; Madison, WI) and four hESC cultures H7, H14 (WiCell) and CM7, CM14, established at CMRC (Laurant et al., 2010), (currently pending approval for addition to the NIH Stem Cell Registry) were used for this study. The cells were grown in StemPro medium (Invitrogen; Carlsbard, CA) on a Matrigel substrate (BD Bioscience; San Jose, CA). The cultures were split mechanically using the StemPro EZ Passage tool (Invitrogen). For miR analysis, confluent cultures were lifted using trypsin and then washed in ice-cold PBS and pellet stored at −80 °C.

Western Blot, Real-time RT-PCR DNA methylation analyses

Thirty micrograms of total cell lysate from hiPSCs or hESCs were loaded per lane in pairs onto a 4–12% Tris-Bis SDS-PAGE (Invitrogen). After transblotting onto an Immobilon membrane (Millipore; Billerica, MA), the membrane was cut into thirds and each section probed for either Nodal (antibody Clone EP2058Y; Epitomics; Burlingame, CA), Lefty (antibody AF746; R&D Systems; Minneapolis, MN) or Cripto-1 (antibody 600-401-997; Rockland; Gilbertsville, PA). The membranes were then stripped and reprobed for actin (antibody MAB1501; Millipore) as a protein loading control. For Real-time RT-PCR, RNA was isolated using TRizol reagent (Invitrogen) and 1 μg reverse transcribed as previously described (Postovit et al., 2008). Real-time RT-PCR was performed as described (Postovit et al., 2008) using *Taq*Man (Applied Biosystems; Carlsbad, California) gene expression human primer/probe sets for *Nodal* (Hs00250630.s1), *Lefty* (Hs009996632.g1) and *Cripto-1* (Hs02339499.g1) and gene levels normalized using *HPRT-1* (433768F). Data were analyzed using Applied Biosystems' Sequence Detection Software (V. 1.2.3) and error bars represent mean gene expression normalized to hESC values, +/−S.D. DNA from hiPSCs and hESCs was extracted by phenol-chloroform, bisulfite converted and sequenced for the *Lefty B* gene CpG island as previously reported (Costa et al., 2009). Six to ten positive clones were sequenced and percentages of DNA methylation were calculated.

miR analysis

Total mRNA isolation from the cell lines was performed with the PureZOL RNA isolation reagent (Bio-Rad; Hercules, CA), according to the manufacturer's instructions. *Taq*Man Low-Density Arrays (TLDA Human MicroRNA Panel v1.0) were used to detect and quantify mature miRs in accordance with the manufacturer's instructions (Applied Biosystems' 7900HT Micro Fluidic Cards). The cards were processed in the ABI 7900 HT Fast Real Time PCR System (Applied Biosystems) and analyzed with Real-Time StatMiner (Integromics; Philadelphia, PA). The difference in miR expression between hiPSCs and hESCs was calculated by the comparative $2^{-\Delta\Delta Ct}$ method with RNU44 and RNU48 as endogenous controls (Livak and Schmittgen, 2001) ($P<0.05$ was considered as significant). Hierarchical clustering was performed by the Ward's method using Pearson's correlation for

miR similarity measure. miRs with ΔCt<5 (RNU48 as endogenous controls) were considered to be at high level of expression.

To verify the accuracy of our TLDA data, we performed individual qRT-PCR experiments for representative miRs using TaqMan miR assays (Applied Biosystems) in triplicates, according to the manufacturer's instructions (RNU48 as endogenous controls). miR expression levels were analyzed as above and the miRs were confirmed to be significantly up-regulated in the hiPSC compare to the hESC lines by the individual qRT-PCR experiments.

RESULTS AND DISCUSSION

This study initially performed a comparative analysis of the major components of the embryonic Nodal signaling pathway in hESCs and hiPSCs. Western blot and Real-time RT-PCR results reveal slightly lower levels of Nodal (a TGF-β family member) and Cripto-1 (Nodal's co-receptor) and a dramatic decrease in Lefty (Nodal's inhibitor and TGF-β family member) in hiPSCs compared with hESCs (Fig. 1A). Based on the unanticipated noteworthy drop in hiPSC's Lefty expression, we performed DNA sequence-based methylation analysis of *Lefty B* CpG island and found increased methylation (Fig. 1A), suggesting silencing of this critical regulator of Nodal. The implications associated with a significantly lower level of Lefty expression in hiPSCs *vs.* hESCs, together with our earlier findings of the re-emergence of aberrant Nodal signaling in metastatic tumor cells in the absence of Lefty (Postovit et al., 2008), prompted us to address a more fundamental question focused on the implications associated with the epigenetic reprogramming of hiPSCs, particularly related to the fidelity of these cells to maintain a stable ESC phenotype.

We pursued a comparison of the expression profiles of 365 microRNAs (miRs) in two hiPSC (fibroblasts reprogrammed with *Oct4*, *Sox2*, *Nanog* and *Lin28*) and four hESC lines, recognizing that specific miRs are known to be associated with oncogenic pathways (Tong et al., 2009). Although the ability of hESCs and hiPSCs to form teratomas in immunocompromised mice is well documented (Yu et al, 2007; Thomson et al. 1998), particularly noteworthy are the observations in chimeric mice derived from iPSCs generated with exogenous *c-myc*, where malignant tumors developed in up to 20% of the mice (Okita et al., 2007) *vs.* mice derived from iPSCs reprogrammed without exogenous *c-myc*, where no tumors have been reported (Wernig et al, 2008). These disparate findings prompted further inquiry into the potential pathways employed by normal cells resulting in pluripotency *vs.* oncogenic transformation.

An unsupervised hierarchical clustering analysis of 157 miRs that were expressed in at least one of the six cell lines tested (Fig.1B-1) revealed 72 miRs expressed at statistically different levels in hiPSCs *vs.* hESCs ($P<0.05$), 31 exhibiting greater than 10-fold difference (Fig. 1B-2; Table 1). Further statistical analysis of the 31 miRs indicated that 15 were expressed at high levels (ΔCt<5), 10 of which have been shown to be cancer related (Fig. 1B-3). Specifically, differential expression of these 10 miRs have been shown to regulate critical checkpoints in Hodgkin's lymphoma, multiple myeloma, and breast, pancreatic and prostatic carcinoma (Tong et al. 2009; Pichiorri et al., 2008; Griether et al., 2010; Mertens-Talcott et al., 2007; Gibcus et al., 2009; Yan et al., 2008). The miR differences found in this study between hiPSCs and hESCs further support the recent findings of Doi and colleagues (Doi et al., 2009), who indicated that the target loci involved in epigenetic reprogramming to pluripotency parallels aberrant oncogenic transformation programming, and advances the observations of Feng and coworkers reporting early senescence of hiPSCs derivatives (Feng et al., 2010). Our investigation also revealed that both hiPSCs fibroblasts -- isolated from either fetal origin (IMR90) or newborn foreskin hiPSCs resulted in a similar miR expression

profile between them as did hESCs miR expression among cell lines of different ethnic origin. Collectively, these data demonstrate cancer hallmarks expressed by hiPSCs, which will require further elucidation for their impact on clinical applications, especially with respect to the fate of precancerous stem cells.

Acknowledgments

The authors wish to thank Drs. Victor Ambrose and Todd Golub for critical reading of the manuscript. Research was supported by NCI CA121205 and CA143869 (MJCH), NHLBI10279457 (VG) and the Maeve McNicholas Memorial Foundation (FFC).

LITERATURE CITED

Chin MH, Mason MJ, Xie W, Volinia S, Singer M, Peterson C, Ambartsumyan G, Aimiuwu O, Richter L, Zhang J, Khvorostov I, Ott V, Grunstein M, Lavon N, Benvenisty N, Croce CM, Clark AT, Baxter T, Pyle AD, Teitell MA, Pelegrini M, Plath K, Lowry WE. Induced pluripotent stem cells and embryonic stem cells are distinguished by gene expression signatures. Cell Stem Cell. 2009; 5(1):111–123. [PubMed: 19570518]

Costa FF, Seftor EA, Bischof JM, Kirschmann DA, Strizzi L, Arndt K, Bonaldo MdeF, Soares MB, Hendrix MJC. Epigenetically reprogramming metastatic tumor cells with an embryonic microenvironment. Epigenomics. 2009; 1(2):387–398. [PubMed: 20495621]

Doi A, Park IH, Wen B, Murakami P, Aryee MJ, Irizarry R, Herb B, Ladd-Acosta C, Rho J, Loewer S, Miller J, Schlaeger T, Daley GQ, Feinberg AP. Differential methylation of tissue- and cancer-specific CpG island shores distinguishes human induced pluripotent stem cells, embryonic stem cells and fibroblasts. Nat Genet. 2009; 41(12):1350–13533. [PubMed: 19881528]

Feng Q, Lu SJ, Klimanskaya I, Gomes I, Kim D, Chung Y, Honig GR, Kim KS, Lanza R. Hemangioblastic derivatives from human induced pluripotent stem cells exhibit limited expansion and early senescence. Stem Cells. 2010; 28(4):704–712. [PubMed: 20155819]

Gibcus JH, Tan LP, Harms G, Schakel RN, de Jong D, Blokzijl T, Möller P, Poppema S, Kroesen BJ, van den Berg A. Hodgkin lymphoma cell lines are characterized by a specific miRNA expression profile. Neoplasia. 2009; 11(2):167–176. [PubMed: 19177201]

Greither T, Grochola LF, Udelnow A, Lautenschläger C, Würl P, Taubert H. Elevated expression of microRNAs 155, 203, 210 and 222 in pancreatic tumors is associated with poorer survival. Int J Cancer. 2010; 126(1):73–80. [PubMed: 19551852]

Knoepfler PS. Deconstructing stem cell tumorigenicity: A roadmap to safe regenerative medicine. Stem Cells. 2009; 27:1050–1056. [PubMed: 19415771]

Laurent LC, Nievergelt CM, Lynch C, Fakunle E, Harness JV, Schmidt U, Galat V, Laslett AL, Otonkoski T, Keirstead HS, Schork A, Park HS, Loring JF. Restricted ethnic diversity in human embryonic stem cell lines. Nat Methods. 2010; 7(1):6–7. [PubMed: 20038950]

Livak KJ, Schmittgen TD. Analysis of relative gene expression data using real-time quantitative PCR and the 2(-Delta Delta C(T)) Method. Methods. 2001; 25(4):402–408. [PubMed: 11846609]

Mertens-Talcott SU, Chintharlapalli S, Li X, Safe S. The oncogenic microRNA-27a targets genes that regulate specificity protein transcription factors and the G2-M checkpoint in MDA-MB-231 breast cancer cells. Cancer Res. 2007; 67(22):11001–11. [PubMed: 18006846]

Okita K, Ichisaka T, Yamanaka S. Generation of germline-competent induced pluripotent stem cells. Nature. 2007; 448(7151):313–317. [PubMed: 17554338]

Pichiorri F, Suh SS, Ladetto M, Kuehl M, Palumbo T, Drandi D, Taccioli C, Zanesi N, Alder H, Hagan JP, Munker R, Volinia S, Boccadoro M, Garzon R, Palumbo A, Aqeilan RI, Croce CM. MicroRNAs regulate critical genes associated with multiple myeloma pathogenesis. Proc Natl Acad Sci USA. 2008; 105(35):12885–12890. [PubMed: 18728182]

Postovit LM, Margaryan NV, Seftor EA, Kirschmann DA, Lipavsky A, Wheaton WW, Abbott DE, Seftor RE, Hendrix MJ. Human embryonic stem cell microenvironment suppresses the tumorigenic phenotype of aggressive cancer cells. Proc Natl Acad Sci USA. 2008; 105(11):4329–4334. [PubMed: 18334633]

Schier AF. Nodal signaling in vertebrate development. Annu Rev Cell Dev Biol. 2003; 19:589–621. [PubMed: 14570583]

Schier AF, Shen MM. Nodal signaling in vertebrate development. Nature. 2000; 403(6768):385–389. [PubMed: 10667782]

Thomson JA, Itskovitz-Eldor J, Shapiro SS, Waknitz MA, Swiergiel JJ, Marshall VS, Jones JM. Embryonic stem cell lines derived from human blastocysts. Science. 1998; 282(5391):1145–1147. Erratum in: Science 282(5395):1827,1998. [PubMed: 9804556]

Tong AW, Fulgham P, Jay C, Chen P, Khalil I, Liu S, Senzer N, Eklund AC, Han J, Nemunaitis J. MicroRNA profile analysis of human prostate cancers. Cancer Gene Ther. 2009; 16(3):206–216. [PubMed: 18949015]

Yan LX, Huang XF, Shao Q, Huang MY, Deng L, Wu QL, Zeng YX, Shao JY. MicroRNA miR-21 overexpression in human breast cancer is associated with advanced clinical stage, lymph node metastasis and patient poor prognosis. RNA. 2008; 14(11):2348–2360. [PubMed: 18812439]

Yu J, Vodyanik MA, Smuga-Otto K, Antosiewicz-Bourget J, Frane JL, Tian S, Nie J, Jonsdottir GA, Ruotti V, Stewart R, Slukvin II, Thomson JA. Induced pluripotent stem cell lines derived from human somatic cells. Science. 2007; 318(5858):1917–1920. [PubMed: 18029452]

Wernig M, Meissner A, Cassady JP, Jaenisch R. c-Myc is dispensable for direct reprogramming of mouse fibroblasts. Cell Stem Cell. 2008; 2(1):10–12. [PubMed: 18371415]

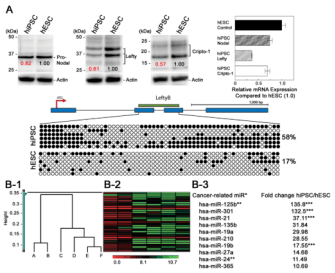

Figure 1. Differences in pluripotent markers and oncogenic-associated miRs in hiPSCs *vs.* hESCs

(A) Upper, Western blot and Real-time RT-PCR analyses of hiPSCs (IRM90-1) and hESCs (H9) for the expression of Nodal, Lefty and Cripto protein (relative values corrected against Actin for protein loading); Right, mRNA expression (normalized to hESC values). Lower, DNA methylation of the *Lefty* B CpG island. **(B-1)** Comparison of miR expression profiles between two hiPSC and four hESC lines. Unsupervised hierarchical clustering of 157 microRNAs (ΔCt, Pearson's correlation, P<0.05): A-hiPSC (Foreskin-1), B-hiPSC (IMR90-1), C-hESC (CM7), D-hESC (H7), E-hESC (CM14), F-hESC (H14). **(B-2)** Supervised hierarchical clustering using 10-fold change between hiPSC and hESC lines as a cutoff (31 miRs-the same order of samples as in **(B-1)** (ΔCt, Pearson's correlation, P<0.05): **(B-3)** Cancer related miRs highly expressed (ΔCt <5) in both hiPSC lines. (*based on literature search; **miR was also found to be differentially expressed between hiPSC and hESC lines [Chin et al., 2009]; ***verified by individual qRT-PCR experiments [P<0.05]).

J Cell Physiol. Author manuscript; available in PMC 2011 November 1.

Table 1

miRs with higher that 10-fold difference between hiPSC and hESC (P<0.05).

miR ID	ΔCt.hiPSC*	ΔCt.hiPSC**	ΔCt.CM7	ΔCt.H7	ΔCt.CM14	ΔCt.H14	P.Value hiPSC/hESC	Fold change hiPSC/hESC
hsa-miR-100	4.69416	6.18674	9.106	10.4526	11.3265	14.421	5.87E-03	59.141657
hsa-miR-107	10.6296	9.01294	14.006	15.6715	10.4502	14.408	3.78E-02	14.051576
hsa-miR-125b	**3.62447**	**3.93389**	**14.298**	**9.76494**	**10.7071**	**8.6904**	**2.74E-03**	**135.85824**
hsa-miR-126	2.2856	5.59768	10.13	8.11429	10.3783	7.1025	8.20E-03	31.772336
hsa-miR-135b	**3.13058**	**2.9034**	**8.2714**	**8.3519**	**8.87317**	**6.5433**	**6.24E-04**	**31.843842**
hsa-miR-146a	4.82376	6.80023	14.006	7.96537	10.6522	14.408	1.85E-02	61.644926
hsa-miR-148b	6.94789	7.45066	14.276	10.5456	9.22546	10.283	2.99E-02	14.755777
hsa-miR-19a	**1.03961**	**0.89319**	**5.62**	**6.49591**	**6.04151**	**5.3333**	**1.63E-04**	**29.987217**
hsa-miR-19b	**−1.21677**	**−2.18826**	**2.1964**	**2.9728**	**2.50776**	**2.0489**	**5.21E-04**	**17.556964**
hsa-miR-203	6.36282	7.5737	14.276	15.5623	12.2474	8.9076	1.62E-02	54.953025
hsa-miR-205	3.57615	4.01991	13.831	4.90553	11.402	8.9448	0.0368032	62.801745
hsa-miR-21	**1.62564**	**3.08243**	**6.623**	**7.20019**	**7.94788**	**8.5**	**4.85E-04**	**37.110229**
hsa-miR-210	**3.43064**	**3.76809**	**7.7933**	**8.59223**	**9.09493**	**8.2604**	**2.05E-04**	**28.558479**
hsa-miR-218	3.17776	4.09403	9.9162	9.03569	10.1291	14.408	2.44E-03	150.79312
hsa-miR-23b	7.60497	7.76488	8.5527	15.7719	16.3	14.545	0.026757647	68.952717
hsa-miR-24	**1.24742**	**2.14878**	**5.0701**	**5.05449**	**5.70204**	**5.056**	**1.06E-03**	**11.491895**
hsa-miR-27a	**3.99271**	**4.74047**	**7.382**	**8.07386**	**9.34138**	**8.1756**	**1.68E-03**	**14.688638**
hsa-miR-27b	5.4428	6.37508	14.298	8.40736	11.3624	9.6495	1.79E-02	32.455943
hsa-miR-29c	8.35607	9.58522	14.328	14.3582	10.3855	14.599	1.39E-02	21.814394
hsa-miR-301	**4.2136**	**3.46591**	**8.0127**	**10.7268**	**16.3988**	**8.4205**	**2.04E-02**	**132.50964**
hsa-miR-324-5p	7.32669	6.84188	11.45	11.3357	11.5308	8.6837	8.49E-03	12.691103
hsa-miR-362	4.96103	6.81756	8.1027	10.3066	9.80054	9.5704	6.43E-03	11.759371
hsa-miR-365	**4.41274**	**4.70499**	**8.0357**	**8.14142**	**8.47349**	**7.2595**	**1.37E-03**	**10.693454**
hsa-miR-367	-1.37627	-2.05992	4.1982	3.86308	3.4638	3.5087	7.05E-05	44.524893
hsa-miR-375	2.47171	6.95772	14.006	9.9749	10.451	6.7039	3.57E-02	47.478107
hsa-miR-449	8.71851	7.88594	14.298	12.2549	10.1219	14.682	1.37E-02	23.213763
hsa-miR-501	6.11818	6.73567	14.298	15.4146	10.8148	14.682	1.03E-03	166.03692
hsa-miR-532	3.28642	5.17148	7.2698	7.85785	8.32335	8.685	2.53E-03	13.977622
hsa-miR-660	3.12787	4.66706	14.013	8.4383	9.67692	8.686	7.35E-03	79.130927

miR ID	ΔCt.hiPSC*	ΔCt.hiPSC**	ΔCt.CM7	ΔCt.H7	ΔCt.CM14	ΔCt.H14	P.Value hiPSC/hESC	Fold change hiPSC/hESC
hsa-miR-7	4.21268	5.67803	8.5316	11.0034	8.56415	9.7348	2.49E-03	22.834218
hsa-miR-9	3.54422	2.82988	6.9939	8.77523	8.71774	7.977	4.50E-04	30.461488

* hiPSC Foreskin-1,

** hiPSC IMR90-1, bold-cancer related miRs from Fig.1B-3.